Stem Cell Reports, Volume *12*

Supplemental Information

SQSTM1/p62-Directed Metabolic Reprogramming Is Essential for Normal Neurodifferentiation

Javier Calvo-Garrido, Camilla Maffezzini, Florian A. Schober, Paula Clemente, Elias Uhlin, Malin Kele, Henrik Stranneheim, Nicole Lesko, Helene Bruhn, Per Svenningsson, Anna Falk, Anna Wedell, Christoph Freyer, and Anna Wredenberg

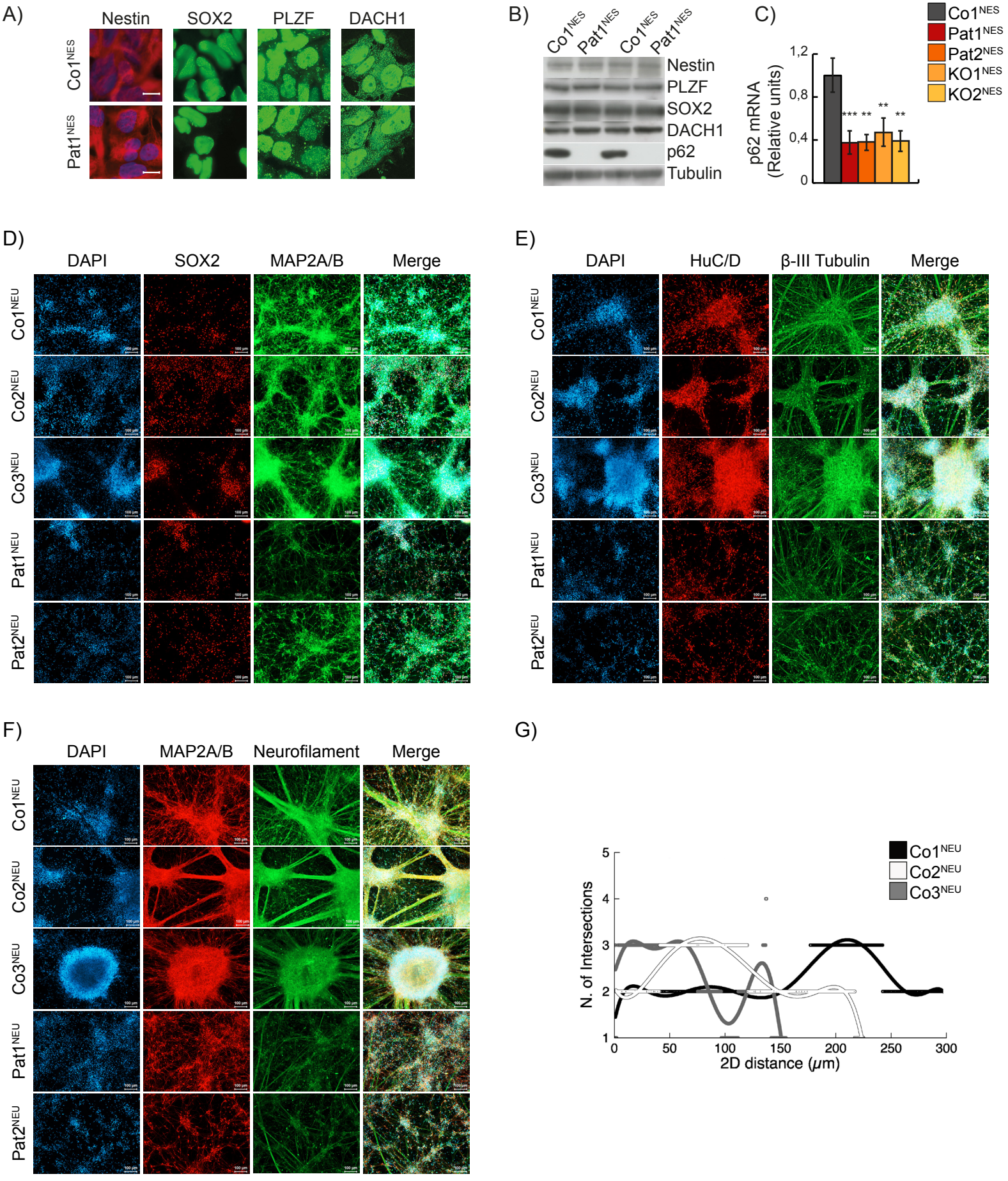
A)
Nestin
SOX2
PLZF
DACH1
Co1NES
Pat1NES
B)
Co1NES
Pat1NES
Co1NES
Pat1NES
Nestin
PLZF
SOX2
DACH1
p62
Tubulin
C)
Co1NES
Pat1NES
Pat2NES
KO1NES
KO2NES
p62 mRNA (Relative units)
1,2
0,8
0,4
0
***
**
**
**
D)
DAPI
SOX2
MAP2A/B
Merge
Co1NEU
Co2NEU
Co3NEU
Pat1NEU
Pat2NEU
E)
DAPI
HuC/D
β-III Tubulin
Merge
Co1NEU
Co2NEU
Co3NEU
Pat1NEU
Pat2NEU
F)
DAPI
MAP2A/B
Neurofilament
Merge
Co1NEU
Co2NEU
Co3NEU
Pat1NEU
Pat2NEU
G)
Co1NEU
Co2NEU
Co3NEU
N. of Intersections
5
4
3
2
1
0
50
100
150
200
250
300
2D distance (μm)

Figure S1

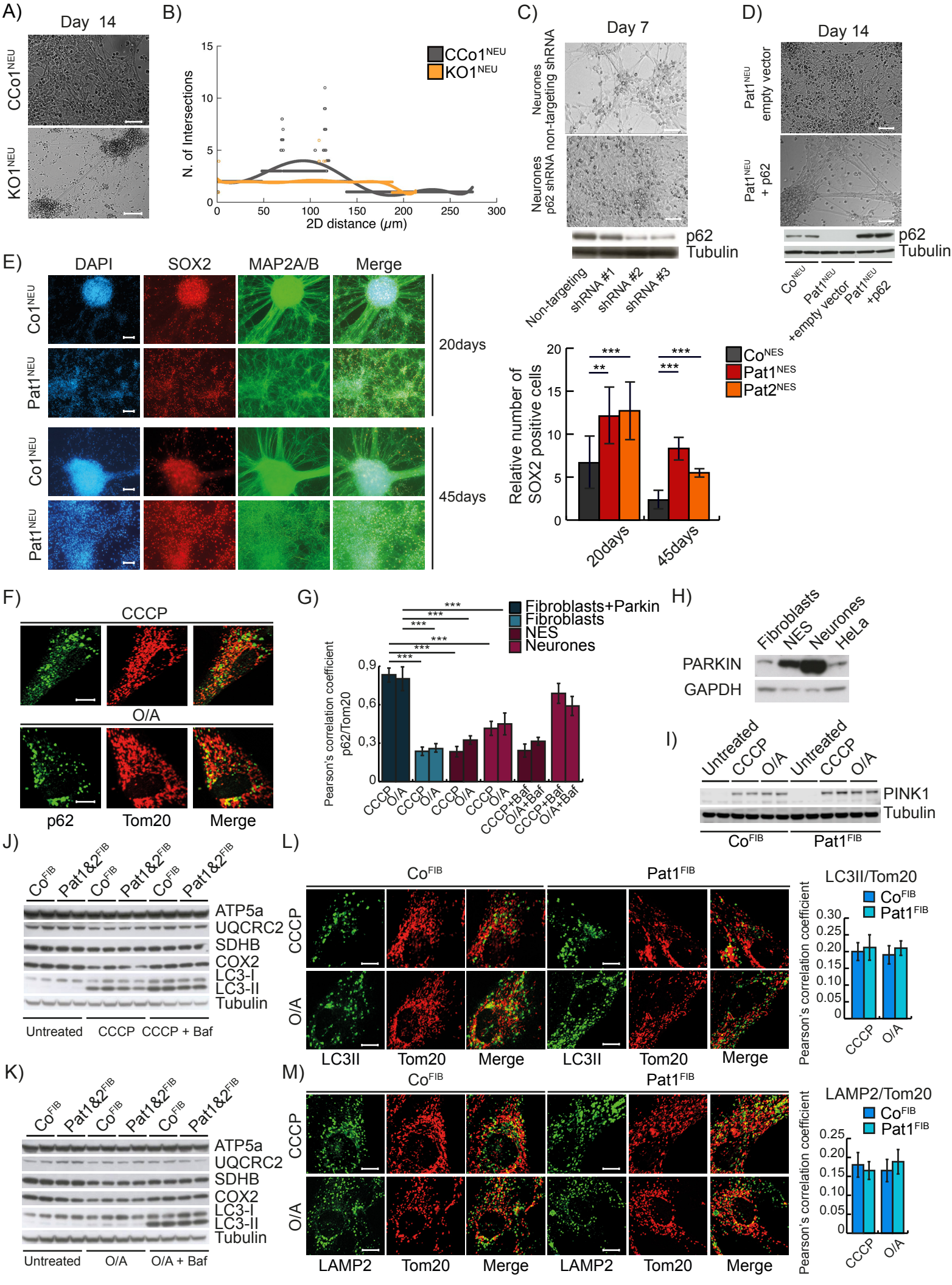
A)
Day 14
CCo1NEU
KO1NEU
B)
CCo1NEU
KO1NEU
N. of Intersections
2D distance (μm)
C)
Day 7
Neurones non-targeting shRNA
Neurones p62 shRNA
p62
Tubulin
Non-targeting
shRNA #1
shRNA #2
shRNA #3
D)
Day 14
Pat1NEU empty vector
Pat1NEU + p62
p62
Tubulin
CoNEU
Pat1NEU +empty vector
Pat1NEU +p62
E)
DAPI
SOX2
MAP2A/B
Merge
Co1NEU
Pat1NEU
20days
45days
Relative number of SOX2 positive cells
CoNES
Pat1NES
Pat2NES
20days
45days
F)
CCCP
O/A
p62
Tom20
Merge
G)
Fibroblasts+Parkin
Fibroblasts
NES
Neurones
Pearson's correlation coefficient p62/Tom20
CCCP
O/A
CCCP+Baf
O/A+Baf
H)
Fibroblasts
NES
Neurones
HeLa
PARKIN
GAPDH
I)
Untreated
CCCP
O/A
PINK1
Tubulin
CoFIB
Pat1FIB
J)
CoFIB
Pat1&2FIB
ATP5a
UQCRC2
SDHB
COX2
LC3-I
LC3-II
Tubulin
Untreated
CCCP
CCCP + Baf
K)
CoFIB
Pat1&2FIB
ATP5a
UQCRC2
SDHB
COX2
LC3-I
LC3-II
Tubulin
Untreated
O/A
O/A + Baf
L)
CoFIB
Pat1FIB
CCCP
O/A
LC3II
Tom20
Merge
LC3II/Tom20
Pearson's correlation coefficient
M)
CoFIB
Pat1FIB
CCCP
O/A
LAMP2
Tom20
Merge
LAMP2/Tom20
Pearson's correlation coefficient

Figure S2

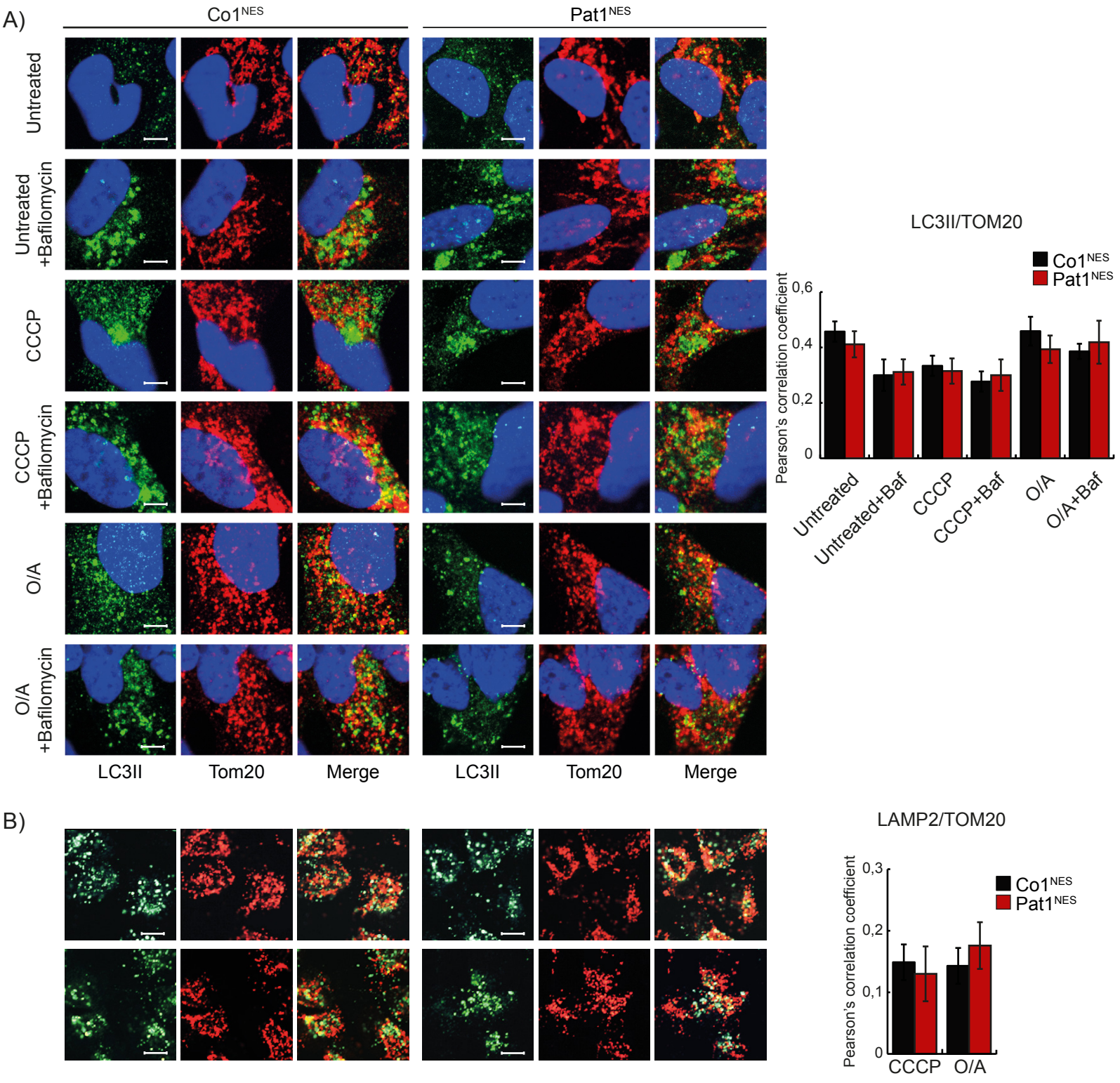
A)
Co1NES
Pat1NES
Untreated
Untreated +Bafilomycin
CCCP
CCCP +Bafilomycin
O/A
O/A +Bafilomycin
LC3II
Tom20
Merge
LC3II/TOM20
Co1NES
Pat1NES
Pearson's correlation coefficient
0,6
0,4
0,2
0
Untreated
Untreated+Baf
CCCP
CCCP+Baf
O/A
O/A+Baf
B)
LAMP2/TOM20
Co1NES
Pat1NES
Pearson's correlation coefficient
0,3
0,2
0,1
0
CCCP
O/A

Figure S3

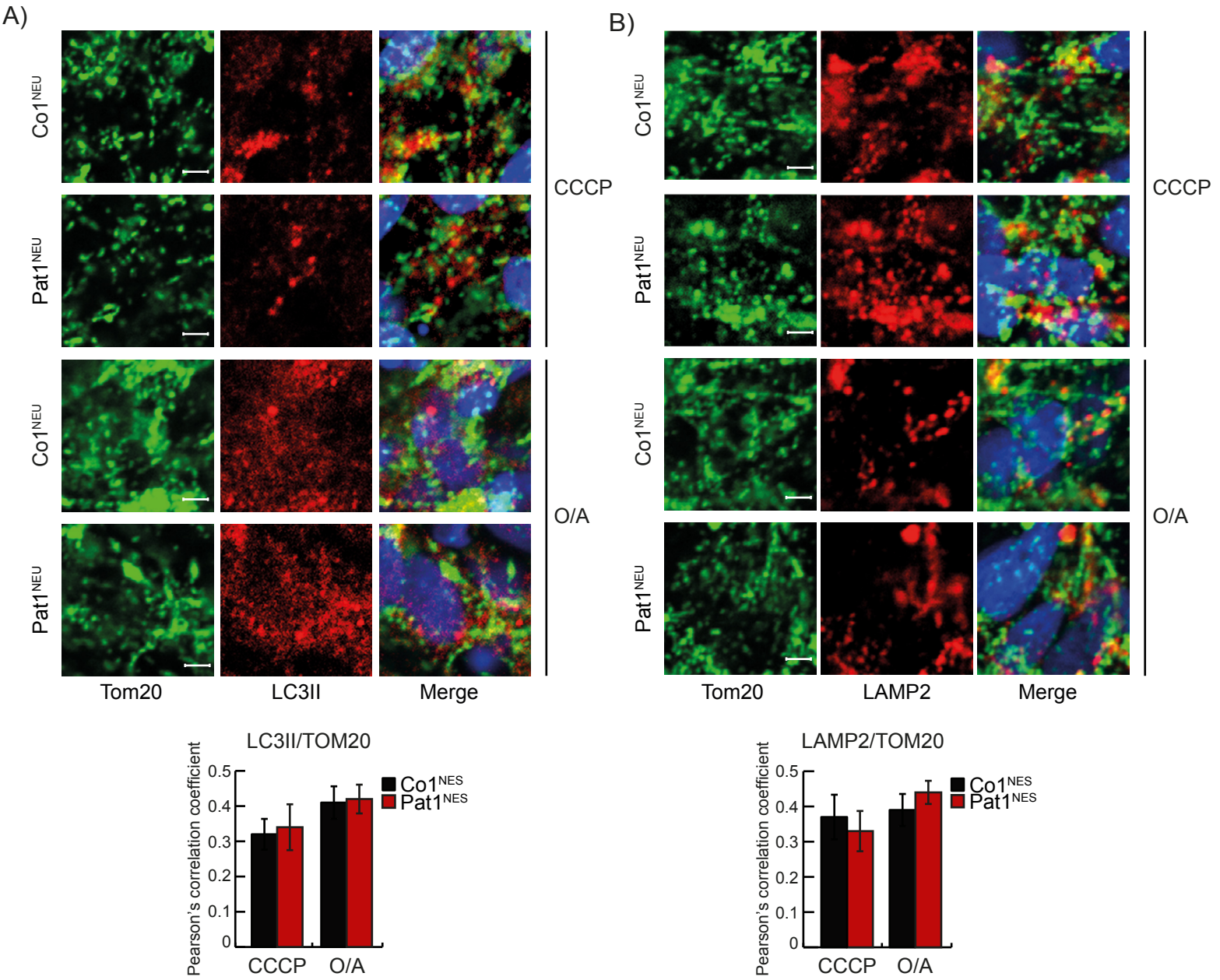
A)
B)
Co1NEU
Pat1NEU
CCCP
O/A
Tom20
LC3II
Merge
LAMP2
LC3II/TOM20
LAMP2/TOM20
Pearson's correlation coefficient
Co1NES
Pat1NES
C)
D)
CCo1NES
KO1NES
GSH (nmol/µg protein)
Day 0
Day 4
mRNA levels (Relative units)
GSS
NRF2
NQO1
GSTM4
TRX1
SOD1
GSR
GCLC
GCLM
xCT
CCo1NES + CCCP
KO1NES + CCCP
E)
Untreated
p62
F)
GPX4
GSTP1
Nqo1
p62
Tubulin
G)
Nqo1 levels (relative units)

Figure S4

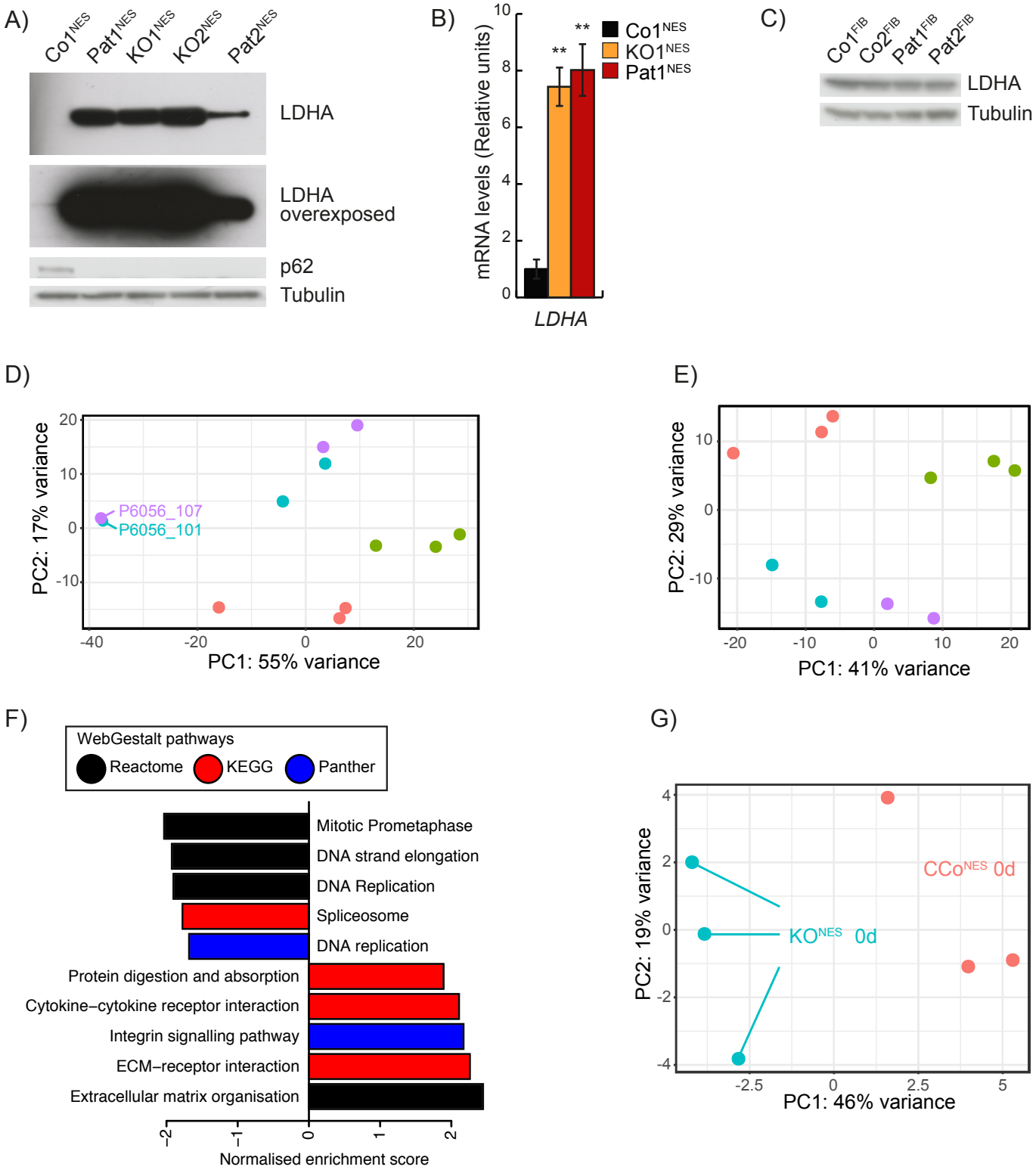
A)
Co1NES
Pat1NES
KO1NES
KO2NES
Pat2NES
LDHA
LDHA overexposed
p62
Tubulin
B)
mRNA levels (Relative units)
Co1NES
KO1NES
Pat1NES
**
**
LDHA
C)
Co1FIB
Co2FIB
Pat1FIB
Pat2FIB
LDHA
Tubulin
D)
PC2: 17% variance
PC1: 55% variance
P6056_107
P6056_101
E)
PC2: 29% variance
PC1: 41% variance
F)
WebGestalt pathways
Reactome
KEGG
Panther
Mitotic Prometaphase
DNA strand elongation
DNA Replication
Spliceosome
DNA replication
Protein digestion and absorption
Cytokine–cytokine receptor interaction
Integrin signalling pathway
ECM–receptor interaction
Extracellular matrix organisation
Normalised enrichment score
G)
PC2: 19% variance
PC1: 46% variance
CCoNES 0d
KONES 0d

Figure S5

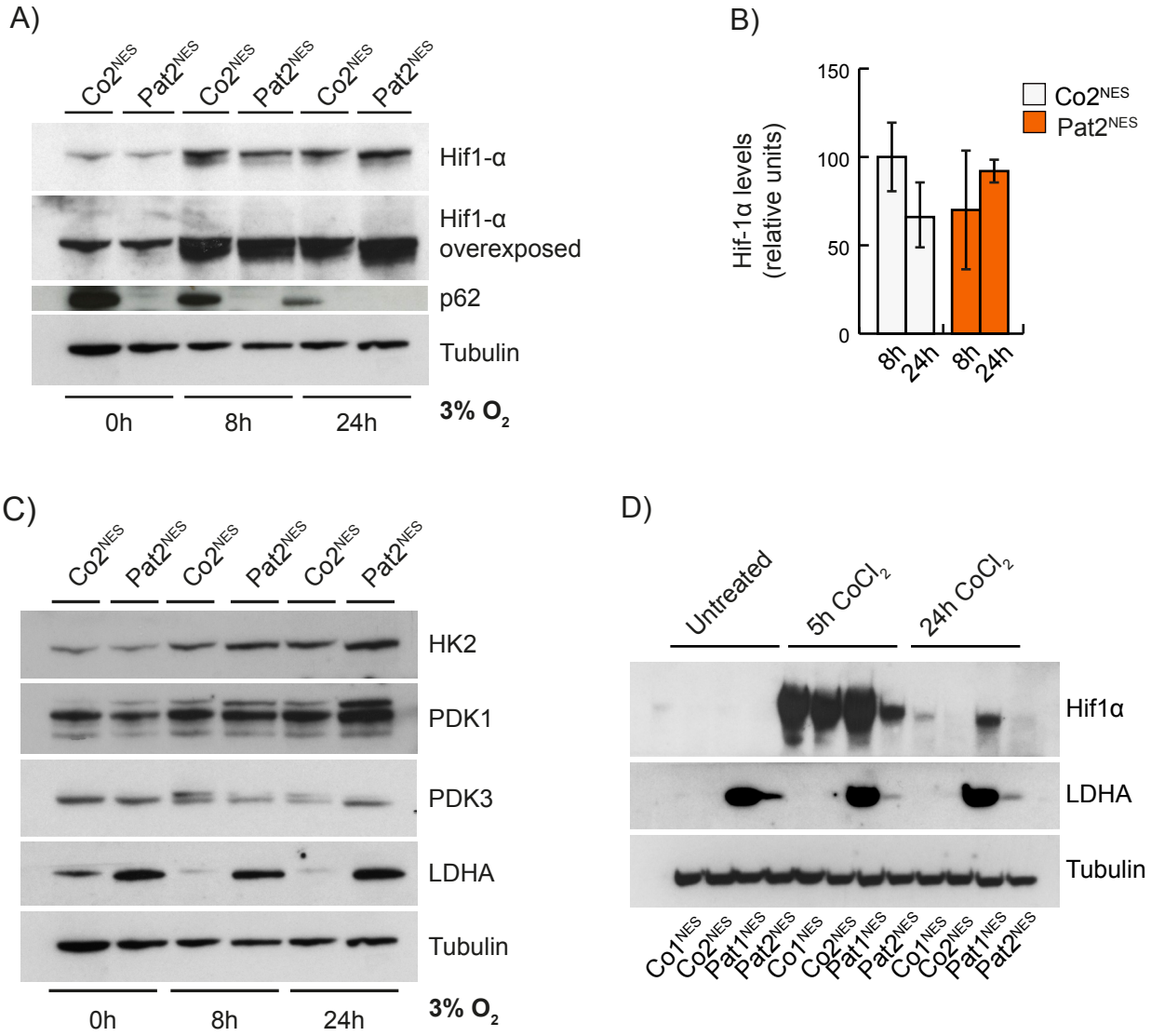
A)
Co2NES
Pat2NES
Co2NES
Pat2NES
Co2NES
Pat2NES
Hif1-α
Hif1-α
overexposed
p62
Tubulin
0h
8h
24h
3% O2
B)
Hif-1α levels
(relative units)
150
100
50
0
Co2NES
Pat2NES
8h
24h
8h
24h
C)
Co2NES
Pat2NES
Co2NES
Pat2NES
Co2NES
Pat2NES
HK2
PDK1
PDK3
LDHA
Tubulin
0h
8h
24h
3% O2
D)
Untreated
5h CoCl2
24h CoCl2
Hif1α
LDHA
Tubulin
Co1NES
Co2NES
Pat1NES
Pat2NES
Co1NES
Co2NES
Pat1NES
Pat2NES
Co1NES
Co2NES
Pat1NES
Pat2NES

Figure S6

SUPPLEMENTARY FIGURES LEGENDS

Figure S1. Characterisation of NES cells. Related to figure 1.
(**A**) Representative fluorescence images of $Co1^{NES}$, $Pat1^{NES}$ immunostained against stem cell markers Nestin, SOX2, PLZF and DACH1. Scale bar: 20 µm. (**B**) Representative western blot analysis of Nestin, SOX2, PLZF and DACH1 in $Co1^{NES}$ and $Pat1^{NES}$ cells. Tubulin was used as a loading control. For (A-B) n=3 independent experiments. (**C**) qRT-PCR analysis of p62 transcript levels in $Co1^{NES}$ (grey), $Pat1^{NES}$ (red), $Pat2^{NES}$ (orange), $KO1^{NES}$ (dark yellow) and $KO2^{NES}$ (light yellow) cells. Data are expressed as mean ± standard deviation (SD) and differences were tested by a two-tailed t-test. ** $p < 0.01$ and *** $p < 0.001$, n=3 independent experiments.
Figure S2. Characterisation of neuronal differentiation. Related to figure 1. (**D**) Representative fluorescence images of $Co1^{NEU}$, $Co2^{NEU}$, $Co3^{NEU}$, $Pat1^{NEU}$ and $Pat2^{NEU}$, immunostained against stem cell marker SOX2 and neuronal marker MAP2A/B at 20 days of differentiation. Scale bar: 100 µm. (**E**) Representative fluorescence images of $Co1^{NEU}$, $Co2^{NEU}$, $Co3^{NEU}$, $Pat1^{NEU}$ and $Pat2^{NEU}$ immunostained against neuronal cell markers HuC/D (red), β-III tubulin (green) at 20 days of differentiation. Scale bar: 100 µm. (**F**) Representative fluorescence images of $Co1^{NEU}$, $Co2^{NEU}$, $Co3^{NEU}$, $Pat1^{NEU}$ and $Pat2^{NEU}$ immunostained against neuronal cell markers MAP2A/B (red), Neurofilament (green) at 20 days of differentiation. Scale bar: 100 µm. (**G**) Linear Sholl analysis representation of 20-days differentiated $Co1^{NEU}$, $Co2^{NEU}$, $Co3^{NEU}$. n=3 independent experiments. Neuronal processes analysed from 25 neuronal bodies.

Figure S2. Characterisation of neuronal differentiation and confocal analysis of mitophagy in fibroblasts. Related to figures 1 and 2.
(**A**) Representative bright field images of $CCo1^{NEU}$ and $KO1^{NEU}$ cells after 14 days of differentiation. (**B**) Linear Sholl analysis representation of 20-days differentiated $CCo1^{NEU}$ and $KO1^{NEU}$. n=3 independent experiments. Neuronal processes analysed from 25 neuronal bodies per line. (**C**) Top: representative bright field images of NES cells transduced with non-targeting shRNAs or p62 shRNA #2 and subjected to 7 days of differentiation process. Bottom: western blot analysis of p62 in $Co1^{NES}$ transduced with non-targeting shRNAs and three different p62 shRNAs. (**D**) Top: representative bright field images of $Pat1^{NES}$ cells transduced with empty pBABE or a pBABE-p62 construct and subjected to 14 days of differentiation. Bottom: western blot analysis of p62 in $Co1^{NES}$ and $Pat1^{NES}$ cells transduced with empty pBABE or pBABE-p62. For C and D tubulin was used as a loading control. Scale bar: 100 µm. n=3 independent experiments. (**E**) Left: representative fluorescence images of $Co1^{NEU}$ and $Pat1^{NEU}$, immunostained against stem cell marker SOX2 (red) and neuronal marker MAP2A/B (green) at 20 and 45 days of differentiation. Scale bar: 100 µm. Right: quantification of the relative number of SOX2 positive cells in $Co1^{NEU}$, $Co2^{NEU}$, $Co3^{NEU}$ (pooled as "Co^{NEU}"), $Pat1^{NEU}$ and $Pat2^{NEU}$ cells after 20 and 45 days of differentiation. Data are expressed as mean ± standard deviation (SD) and differences were tested by a two-tailed t-test. ** $p < 0.01$, *** $p < 0.001$. n=3 independent experiments. **(F)** Representative confocal images of Co^{FIB} treated for 2h with CCCP (20 µM) (top) or O/A (10 µM / 1 µM) (bottom). Fibroblasts are immunostained against Tom20 (red) and p62 (green). (**G**) Graphs represent the quantification of Pearson's correlation coefficient between p62 and Tom 20 in fibroblasts overexpressing Parkin, fibroblasts, NES cells and 14-days differentiated neurones. Cells were treated for 2h with CCCP (20 µM for fibroblasts and 10 µM for NES and neurones) or O/A (10 µM / 1 µM for fibroblasts and 5 µM / 1µM for NES and neurones) and with 50 nM bafilomycin. Data are presented as mean ± standard deviation (SD) and differences were tested by a two-tailed t-test. *** $p < 0.001$, n=3 independent experiments. 25 cells per experiment were analysed to calculate Pearson's correlation coefficient. **(H)** Representative western blot analysis of Parkin in fibroblasts, NES cells, 14-day differentiated neurones and HeLa cells. n=2 independent experiments. **(I-K)** Representative western blot analysis in Co^{FIB}, $Pat1^{FIB}$ and $Pat2^{FIB}$ treated for 24h with CCCP (20 µM) or O/A (10 µM / 1 µM) and for 2h with 50nM bafilomycin. Tubulin was used as a loading control. n=3 independent experiments. (**L, M**) Representative confocal images of Co^{FIB} and $Pat1^{FIB}$ treated for 24h with CCCP (20 µM) or O/A (10 µM / 1 µM) immunostained against LC3II (green) and Tom20 (red) in (L) or against LAMP2 (green) and Tom20 (red) in (M). Graphs represent the quantification of Pearson's correlation coefficient between the analyzed proteins. Data are presented as mean ± standard deviation (SD) and differences were tested by a two-tailed t-test. n=3 independent experiments. 25 cells per experiment were analysed to calculate Pearson's correlation coefficient. Scale bars: F 20 µm, L and M 5 µm.

Figure S3. Confocal analysis of mitophagy in NES cells. Related to figure 2.
(**A**) and (**B**) Left: representative confocal images of $Co1^{NES}$ and $Pat1^{NES}$ treated with CCCP (10 µM) and O/A (10 µM / 1 µM) for 12 hours, with or without 50 nM bafilomycin. NES cells were immunostained against LC3II (green), Tom20 (red) and DAPI (blue) in (A) or LAMP2 (green), Tom20 (red) and DAPI (blue). Right: graphs representing the quantification of Pearson's correlation coefficient between the analyzed proteins. Data are presented as mean ± standard deviation (SD). n=3 independent experiments. 25 cells per experiment were analysed to calculate Pearson's correlation coefficient. Scale bars: 20 µm.

Figure S4. Confocal analysis of mitophagy in neurons and differential antioxidant behaviour in NES cells lacking p62. Related to figures 2 and 3.
(**A**) and (**B**) Representative confocal images of $Co1^{NEU}$ and $Pat1^{NEU}$ differentiated for 14 days and treated with CCCP (10 μM) and O/A (10 μM / 1 μM) for 12 hours. Neurones were immunostained against LC3II (red), Tom20 (green) and DAPI (blue) in (A) or LAMP2 (red), Tom20 (green) and DAPI (blue). Right: graphs representing the quantification of Pearson's correlation coefficient between the analyzed proteins. Data are presented as mean ± standard deviation (SD). n=3 independent experiments. 25 cells per experiment were analysed to calculate Pearson's correlation coefficient. Scale bars: 20 μm. (**C**) Quantification of reduced glutathione levels in undifferentiated and 4 days differentiated $CCo1^{NES}$ (grey) and $KO1^{NES}$ (orange). Data are presented as mean ± standard deviation (SD) and differences were tested by a two-tailed t-test. * $p < 0.05$, n=3 independent experiments. (**D**) qRT-PCR analysis in untreated or treated with 10 μM CCCP for 6 hours $CCo1^{NES}$ (grey) and $KO1^{NES}$ (orange). Beta-actin was used as endogenous control. n=2 independent experiments. (**E**) Representative confocal images of NES cells treated for 6 hours with 10 μM CCCP or 5 μM oligomycin and 1 μM antimycin, followed by immunostaining against p62. n=3 independent experiments. Scale bar 10 μm. (**F**) Representative western blot analysis of GPX4, GSTP1, NQO1 and p62 in $Co1^{NES}$ and $Pat1^{NES}$ cells. Tubulin was used as a loading control. n=3 independent experiments. (**G**) Quantification of NQO1 levels from (F). Data are presented as mean ± standard deviation (SD) and differences were tested by a two-tailed t-test. * $p < 0.05$, n=3 independent experiments**.**

Figure S5. Western blot and qPCR analysis of LDHA in NES cells and fibroblasts and quality control of high-throughput data. Related to figure 4 and 5.
(**A**) Representative western blot analysis of LDHA and p62 in $Co1^{NES}$, $Pat1^{NES}$, $KO1^{NES}$, $KO2^{NES}$ cells and $Pat2^{NES}$. Tubulin was used as a loading control. n=3 independent experiments. (**B**) qRT-PCR analysis of LDHA transcript levels in $Co1^{NES}$ (grey), $KO1^{NES}$ (dark yellow) and $Pat1^{NES}$ (red) cells. Beta-actin was used as endogenous control. Data are expressed as mean ± standard deviation (SD) and differences were analysed by a two-tailed t-test. ** $p < 0.01$, n=3 independent experiments. (**C**) Representative western blot analysis of LDHA in two fibroblast control lines, $Pat1^{FIB}$ and $Pat2^{FIB}$. Tubulin was used as a loading control. n=3 independent experiments. (**D**) Principal component analysis of undifferentiated (0d) and differentiated (4d) control CCo^{NES} and KO^{NES} transcriptomes. Two outlier samples are labeled P6056_101 and P6056_107. (**E**) Principal component analysis of undifferentiated (0d) and differentiated (4d) control CCo^{NES} and KO^{NES} transcriptomes, excluding the outlier samples identified in (A). (**F**) Gene Set Enrichment Analysis (GSEA) against pathways in WebGestalt of the outlier transcriptome samples identified in (A) compared to all other samples. (**G**) Principal component analysis of undifferentiated (0d) CCo^{NES} and KO^{NES} proteomes.

Figure S6: Physiological oxygen concentration reveals a pro-glycolytic metabolism in the absence of p62. Related to figure 6.
(**A**) Representative western blot analysis of Hif-1α and p62 steady-state levels in $Co2^{NES}$ and $Pat2^{NES}$ cells, cultured for 0, 8 or 24h at 3% O2. Tubulin was used as a loading control. n=3 independent experiments. (**B**) Quantification of (A). Data are expressed as mean ± standard deviation (SD). n=3 independent experiments. (**C**) Representative western Blot analysis of HK2, PDK1, PDK3 and LDHA as in (A). Tubulin was used as a loading control. n=3 independent experiments. (**D**) Representative western blot analysis of Hif-1α and LDHA in $Co1^{NES}$, $Co2^{NES}$, $Pat1^{NES}$ and $Pat2^{NES}$ cultured for 0, 5 or 24h in the presence of 200 μM CoCl2. Tubulin was used as loading control. n=5 independent experiments.

Table S2. qPCR primer sequences.

Species	Gene (Forward/Reverse)	Sequence (5´-3´)
Human	GCLC forward	TGTCTCCAGGTGACATTCCA
Human	GCLC reverse	GCCTCGGTAAAAGGGAGATG
Human	GCLM forward	CACAGCGAGGAGGAGTTTC
Human	GCLM reverse	TGATTCTACAATGAACAGTTTTGCA
Human	GPX1 forward	TTCCCGTGCAACCAGTTT
Human	GPX1 reverse	AGGGAATTCAGAATCTCTTCGTT
Human	GPX4 forward	TACGGACCCATGGAGGAG
Human	GPX4 reverse	CCACACACTTGTGGAGCTAGAA
Human	GSR forward	TTTACCCCGATGTATCACGC
Human	GSR reverse	TTCATCACACCCAAGTCCCT
Human	GSS forward	TCGTCTCTTTGACATCCACA
Human	GSS reverse	TTCGATCTGTTTCAGGGCTG
Human	GST forward	GCTACAGCCCTGACTTTGAG
Human	GST reverse	AGGTGATCTTGTCTCCAACA
Human	GSTA1 forward	GGTGACAGCGTTTAACAAAGC
Human	GSTA1 reverse	CCGTGCATTGAAGTAGTGGA
Human	GSTK1 forward	TTTGGCTCTGACCGGATG
Human	GSTK1 reverse	CACGGCTGGAGGTATAGGG
Human	GSTP1 forward	TCCCTCATCTACACCAACTATGAG
Human	GSTP1 reverse	GGTCTTGCCTCCCTGGTT
Human	LDHA forward	AACATGGCAGCCTTTTCCTT
Human	LDHA reverse	TAAGACGGCTTTCTCCCTCT
Human	Nqo1 forward	CACTGGTGGCAGTGGCTC
Human	Nqo1 reverse	CCAATGCTATATGTCAGTTGAGG
Human	Nrf2 forward	GACGGTATGCAACAGGACA
Human	Nrf2 reverse	TTGAGGGTATAGATGAGTAAAAATGAT
Human	p62 forward	TACGACTTGTGTAGCGTCTG
Human	p62 reverse	CGTGTTTCACCTTCCGGAG
Human	SOD1 forward	TGACAAAGATGGTGTGGCC
Human	SOD1 reverse	TTCATTTCCACCTTTGCCCA
Human	Trx1 forward	GTGGGCCTTGCAAAATGATC
Human	Trx1 reverse	GGCATGCATTTGACTTCACA
Human	xCT forward	TTTGGAGCTTTGTCTTATGCTG
Human	xCT reverse	GAGTTCCACCCAGACTCGTA

STAR METHODS

CONTACT FOR DETAILS AND RESOURCE SHARING

Further information and requests for resources and reagents should be directed at: Anna Wredenberg (anna.wredenberg@ki.se).

EXPERIMENTAL MODELS AND SUBJECTS DETAILS

Fibroblasts, HeLa and Phoenix-AMPHO cells

Human primary skin fibroblasts (passage 4 to 12) were taken from patients II:1 (Pat1, female) at 30 years of age and II:4 (Pat2, male) 17 years of age at the time of biopsy. The patients were born healthy to consanguineous parents of Kurdish descent and have been previously described in family 4 of (Haack et al., 2016), HeLa cells and Phoenix-AMPHO (ATCC) cells (passage 4 to 10) were cultured at 37°C in a 5% CO_2 atmosphere in DMEM-Glutamax (Thermo Fisher Scientific) media containing 25 mM glucose, 10% FBS (Thermo Fisher Scientific) and 1 mM sodium pyruvate (Thermo Fisher Scientific). Experiments were performed with cells cultured to 80%–90% confluency. Medium was changed regularly and cells were passaged using trypsin (Thermo Fisher Scientific).

Reprogramming of fibroblasts

Fibroblasts were reprogrammed using integration free Sendai virus-vector-mediated reprogramming (CytoTune™-iPS 2.0 reprogramming kit, Thermo Fisher Scientific). Fibroblasts were seeded at a density of 2.5 X 10^4 cells/cm^2. The following day the cells were transduced using the Sendai virus according to the manufacturer's protocol. Seven days after transduction the cells were passaged using Trypsin-EDTA (0.05%) (Thermo Fisher Scientific) to a laminin-521 (Biolamina) coated plate at a density of 1.9 x 10^3 cells/cm^2 in Essential 8TM medium (Thermo Fisher Scientific) containing 5 µM of Y27632 rho-kinase inhibitor (ROCKi) (Millipore). Emerging iPS cell colonies were manually picked for the first passage and then enzymatically passaged as single cells as described below.

Human induced pluripotent stem (hiPS) cells

hiPS cells were cultured on human recombinant Laminin-521 (Biolamina) in Essential 8^{TM} medium (Thermo Fisher Scientific). The cells were enzymatically passaged as single cells, using TrypLE Select 1x (Thermo Fisher Scientific) and seeded in Essential 8^{TM} medium (Thermo Fisher Scientific) containing 10 µM of Y27632 rho-kinase inhibitor (ROCKi) (Millipore).

Neural induction of induced pluripotent stem cells

The neural induction protocol is based on (Chambers et al., 2009). Approximately 3.8 x 10^4 hiPS cells/cm^2 were seeded in a well of a Laminin-521 coated tissue culture plate with 10 µM of ROCKi in Essential 8^{TM} medium. The day after seeding medium was changed to 80% DMEM/F12+GlutaMax (Thermo Fisher Scientific) plus 20% Knockout serum replacement (KSOR) medium (Thermo Fisher Scientific), Non-essential Amino Acids (Thermo Fisher Scientific), 2-mercaptoethanol (Thermo Fisher Scientific), Penicillin-streptomycin (Thermo Fisher Scientific) with 10 nM of SB-431542 (StemCell Technologies), 500 ng/mL of Noggin (PeproTech) and 10 nM CHIR 99021 (StemCell Technologies). Medium was changed daily. SB421542 was omitted from the medium after 5 days of differentiation and KSOR medium was progressively replaced by adding increasing levels of N2B27 medium, containing, 50% DMEM/F12 GlutaMax, 50% Neurobasal (Thermo Fisher Scientific), 2-mercapthoethanol, N-2 Supplement (100X) 5 µl/ml (Thermo Fisher Scientific), B-27 Supplement (50X) 10 µl/ml

(Thermo Fisher Scientific) and Penicillin-streptomycin (25%, 50%, 75% and 100%). At the 12th day of differentiation the cells were passaged and introduced to NES culture conditioned conditions.

Neuroepithelial-like stem (NES) cells

The generation of NES cells has previously been described (Falk et al., 2012; Koch et al., 2009). NES cells (passage 15 to 50) were cultured on 100 µg/ml poly-ornithine/ 2 µg/ml laminin2020-coated culture dishes (both (Sigma-Aldrich)), in DMEM/F-12 GlutaMax (Thermo Fisher Scientific) media containing 17 mM glucose, 100 units/ml penicillin-streptomycin (Thermo Fisher Scientific), N-2 Supplement (1:100) (Thermo Fisher Scientific), B-27 Supplement (1:1000) (Thermo Fisher Scientific), 10 ng/µl bFGF (Thermo Fisher Scientific) and 10 ng/µl EGF (Peprotech) at 37°C in a 5% CO_2 atmosphere. Three-fourths of the media was exchanged daily. Cells were trypsinised using TrypLE Express 1x (Thermo Fisher Scientific). Neuronal differentiation was induced by removing the growth factors bFGF and EGF from the medium and increasing the B-27 Supplement concentration to 1:100. The culture media was exchanged as described above. Control NES cell lines were derived from one male (Co1, C3 in (Wu et al., 2014)) and one female (Co2, AF22 in (Falk et al., 2012)) donors and have been previously described (Falk et al., 2012; Wu et al., 2014). A third control line was introduced (Co3), isolated from another female donor.

Hypoxia experiments were performed in a 3% oxygen concentration incubator for the indicated time periods.

Generation of p62 knockout NES cells by CRISPR/Cas9 gene editing

The p62 locus of control NES cells (Co1) was targeted by CRISPR/Cas9 gene editing technology, as previously described (Cong et al., 2013). In short, pX335-U6-Chimeric_BB-CBh-hSpCas9n (D10A) plasmids (pX335-U6-Chimeric_BB-CBh-hSpCas9n(D10A) was a gift from Feng Zhang (Addgene plasmid # 42335)), with or without the p62 guide RNA sequence (targeting sequences are described in the key resource table), were nucleofected into control NES cells, using a 4D-Nucleofector™ System (Lonza). After nucleofection, cells were seeded in p35 dishes in conditioned NES cell media, at a 10 cell / well density. Following expansion, single clones were picked, using cloning cylinders (Sigma-Aldrich) and screened by Western blot analysis for the absence of p62 using SQSTM1/p62 antibodies (Cell Signaling Technology). Two CRISPR control (CCo1^{NES} and CCo2^{NES}) or p62-deficient (KO1^{NES} and KO2^{NES}) cell clones were used for further analysis.

METHOD DETAILS

Retroviral production and NES cells transduction

For overexpression experiments, p62 cDNA was cloned into pBABE-Puro. For silencing experiments, a p62 shRNA (Origene) or a non-targeting 29-mer scrambled shRNA cassette (Origene) were cloned in pGFP-V-RS. Overexpression and silencing of p62 in control NES and Pat1^{NES} cells were performed by retroviral transduction of the corresponding plasmids.

For production of retrovirus, Phoenix-AMPHO cells (ATCC) were treated for 1h with 25 µM chloroquine (Sigma-Aldrich) and transfected using calcium chloride (Sigma-Aldrich) following manufacturer's instructions. After 7 hours fresh medium was added. Medium was harvested and filtered 24 hours and 48 hours after transfection. Retrovirus-containing medium was concentrated, using a Retro-X™ Concentrator (Clontech) following manufacturer's instructions and resuspended in 0.15% BSA. NES cells were transduced after addition of 5 µg/ml polybrene (Sigma-Aldrich).

Western Blotting

Cells were harvested by trypsinisation and pellets were lysed using RIPA buffer (150 mM NaCl, 1% Triton x-100, 1% Sodium deoxycholate, 0.1% SDS, 1 mM EDTA and 50 mM Tris-HCl pH 7.4) followed by sonication. Whole-cell protein extracts were separated using Novex NuPAGE SDS-PAGE gel system (Thermo Fisher Scientific) and transferred to polyvinylidene difluoride membranes (Millipore), using 25 mM Tris, 192 mM glycine, pH 8.3 and 20% methanol. Membranes were blocked with 5% skim milk in TBS-T (25 mM Tris, 140 mM NaCl, 1% Tween 20, pH 7.4). Primary antibodies were incubated for at least 15h at 4°C. Primary antibodies used were: SQSTM1/p62 (Cell Signaling Technology, 5114S), Tom20 (Santa Cruz Biotechnology, SC-17764), LC3II (Cell Signaling Technology, 3868S, Sigma-Aldrich, L8918), PARKIN (Abcam, ab15954), KEAP1 (Cell Signaling, 4678S), GAPDH (Santa Cruz Biotechnology, SC-20357), Hif-1α (Cell Signaling Technology, 14179S), α-Tubulin (Sigma-Aldrich, T6199), PINK1 (Cell Signaling Technology, 6946), LDHA (Cell Signaling Technology, 2012), HK2 (Cell Signaling Technology, 2106), Phospho-p70 S6 Kinase (Thr389) (Cell Signaling Technology, 9234), p70 S6 Kinase Antibody (Cell Signaling Technology, 9202), c-Myc (Cell Signaling Technology, 5605), total OXPHOS Human Antibody Cocktail (Abcam, ab110411), MAP2A/B (Millipore, MAB3418), HuC/D (Thermo Fisher Scientific, A-21271), PDK1 (Cell Signaling Technology, 30625), PDK3 (Sigma-Aldrich, HPA046583), Nestin (R&D Systems, MAB1259), PLZF (Thermo Fisher Scientific, MA5-15667), DACH1 (ProteinTech, 10914-1-AP), NQO1 (Cell Signaling Technology, 622625), GPX4 (R&D Systems, MAB5457), GSTP1 (Cell Signaling Technology, 3369) and NRF2 (Abcam, ab31163). Membranes were washed and incubated for 2h at RT with the appropriate secondary antibody at a 1:4000 dilution. Secondary antibodies used in this study were: horseradish peroxidase-conjugated anti-rabbit (GE Healthcare, NA9340), anti-mouse (GE Healthcare, NA9310) or anti-goat (Santa Cruz Biotechnology, SC-2020). Western blots were visualised using Clarity Western ECL solution (Bio-Rad), following manufacturer's instructions.

RNA isolation, RT-PCR and quantitative PCR

Total RNA was extracted using TRIzol (Thermo Fisher Scientific), followed by DNase-treatment using TURBO DNA-*free* kit (Thermo Fisher Scientific). 250 ng of RNA were reverse-transcribed using a High-capacity cDNA Reverse Transcription Kit (Applied Biosystems). Quantitative PCR analysis was performed using a Quant Studio 6 Flex instrument and Platinum SYBR Green qPCR supermix-UDG (Thermo Fisher Scientific). Gene expression was normalised to the house-keeping gene actin. Primers are listed in Table S2.

Detection of reactive oxygen species and measurement of glutathione levels

NES cells or NES cells subjected to differentiation for 4 days were incubated at 37°C for 30 minutes with 1 μM CM-H_2DCFDA (Thermo Fisher Scientific). Images were taken using a Carl Zeiss fluorescence microscope. ImageJ software was used for signal intensity analysis.

Glutathione levels were measured in undifferentiated and 4-days differentiated NES cells, using the Glutathione assay kit (Sigma-Aldrich) following manufacturer's instructions.

Immunocytochemistry, confocal microscopy and bright field microscopy

For PARKIN overexpression experiments, fibroblasts were nucleofected using a YFP-PARKIN plasmid (YFP-PARKIN was a gift from Richard Youle (Addgene plasmid # 23955)). 46h later, the fibroblasts were treated with 20 μM CCCP (Sigma-Aldrich) or 10 μM oligomycin and 1 μM antimycin and fixed 2h later using the following protocol.

Fibroblasts, NES cells or neurones were cultured on 1,5 mm cover-slips as described above and fixed for 20 min using 3% paraformaldehyde (VWR) at RT. Permeabilisation and blocking was performed using a combination of saponin 0,1% (Sigma-Aldrich), 1% BSA (Sigma-Aldrich) in PBS for 1 hour. Primary antibodies TOM20 (Santa Cruz Biotechnology, SC-17764), SQSTM1 (Santa Cruz Biotechnology, SC-28359), LAMP2 (Southern Biotech, 9840-01), LC3II (MBL International, M152-3), Beta-3 Tubulin (Sigma-Aldrich, T8578) MAP2A/B (Millipore, MAB3418), Neurofilament (Sigma-Aldrich, N4142), HuC/D (Thermo Fisher Scientific, A-21271), Nestin (R&D Systems, MAB1259), SOX2 (Cell Signaling Technology, 3579S), PLZF (Thermo Fisher Scientific, MA5-15667) and DACH1 (ProteinTech, 10914-1-AP) were diluted in PBS with 1% BSA and incubated overnight. After washing, cells were incubated for 1h with secondary antibodies Alexa Fluor® 488 (Thermo Fisher Scientific, A-11017 (mouse) or A-11034 (rabbit)), Alexa Fluor® 568 (Thermo Fisher Scientific, A-11031 (mouse) or A-11036 (rabbit)) or Alexa Fluor® 633 (Thermo Fisher Scientific, A-21052 (mouse) or A-21071 (rabbit)) at a 1:1000 dilution. Cells were mounted with ProLong® Diamond Antifade Mountant (Thermo Fisher Scientific) and 0.01 µg/ml DAPI (Sigma-Aldrich, D9542), where appropriate. A Nikon Ti-E inverted point scanning confocal microscope A1R Si was used for image acquisition. A Carl Zeiss bright field microscopy was used for neuronal image acquisition during differentiation experiments. ImageJ software was used for image quantification.

Cell viability test

MTT (3-(4,5-dimethylthiazol-2-yl)-2,5-diphenyltetrazolium bromide, Sigma-Aldrich) assays were used to monitor cell growth in the presence or absence of CCCP and NAC. Briefly, NES cells were treated for 15h with 10 µM CCCP and/or 1 mM NAC, followed by 90 min incubation in 300 µg/ml of MTT in phenol-free DMEM-Glutamax (Thermo Fisher Scientific) at 37°C. Cells were incubated for 10 min in 400 µl of DMSO (Sigma-Aldrich). 100 µl aliquots were used to measure emission at 570 nm and 630 nm, using a Infinite200 PRO multimode reader (TECAN).

Mitophagy assays

Fibroblasts were treated for 24 hours with 20 µM CCCP (Sigma-Aldrich), 10 µM oligomycin and 1 µM antimycin or 50 nM bafilomycin (Sigma-Aldrich). NES cells or neurones differentiated for 14 days were treated for 12 hours with 10 µM CCCP (Sigma-Aldrich) or 10 µM oligomycin and 1 µM antimycin. Cells were immunostained followed by confocal visualisation or harvested for Western blot and qRT-PCR analysis.

Mitochondrial function analysis

Mitochondrial respiratory chain enzyme activities were determined as previously described (Wibom et al., 2002). Mitochondrial oxygen consumption measurements of NES cells were performed on intact cells, using an Oroboros oxygraph (Oroboros Instruments GmbH). Maximal respiration was measured by titration of mitochondrial uncoupler CCCP or 2,4-Dinitrophenol (DNP).

RNAseq analysis

Total RNA from CCo1&2^{NES} and KO1&2^{NES} clones at 0 or 4 days differentiation was obtained as previously described. RNA quality was confirmed using a Bioanalyser 2100 (Agilent). Samples with a minimum RNA integrity number (RIN) of 8.5 were used. Sequencing was performed using Illumina HiSeq 2500, High Output V4 chemistry, PE (paired-end) 2x125bp in 1 lane. The library method used was Illumina TruSeq Stranded mRNA, Poly-A selection (200 ng used for each library). Sequencing was performed by the SciLife Laboratory NGI core facility (Science for Laboratories, Stockholm, Sweden). The reads were mapped using Tophat2 (Kim et al., 2013)

to the human reference assembly, version GRCh38. Principal component analysis of the transcriptomic data from all samples showed that KO3^{NES} did not cluster with its corresponding genetic matches both in the undifferentiated and differentiated state (Figure S5D and E). This clone showed poor growth in culture, and further inspection revealed that DNA replication pathways were repressed (Figure S5F). We removed this clone from all analysis, as it probably was compromised during CRISPR/Cas9 gene editing and/or expansion.

Proteomic analysis

Proteomics analysis was performed on control NES cells, KO1&2^{NES}, CCo1&2^{NES} as wells as Pat1^{NES} cells. Samples were lysed by the addition of ProteaseMax/Urea and sonicated. Peptides were separated on a homemade C18 column, 25 cm (Silica Tip 360 µm OD, 75 µm ID, New Objective, Woburn, MA, USA) with a 120 min gradient at a flow rate of 300 nl/min. The gradient went from 5-26% of buffer B (2% acetonitrile, 0.1% formic acid) in 120 min and up to 95% of buffer B in 5 min and injected onto the LC-MS/MS system (UltimateTM 3000 RSLCnano chromatography system and Q Exactive Plus Orbitrap mass spectrometer (Thermo Fisher Scientific). Proteomics analysis was performed by the Karolinska Institute proteomics core facility. Analysis of principal component one and two did not reveal outliers (Figure S5G), therefore all samples were included for further analysis.

Neuronal morphology analysis

Neuronal body area and neuronal processes number and width emerging from neuronal bodies were measured using ZEN 2011 software. Images were acquired using Axio Imager2 fluorescence microscope from Carl Zeiss. For the number of neuronal processes, a minimum threshold of 10 µm width was introduced in order to clarify the morphological changes found.

Sholl analysis

Sholl analysis was performed with Simple Neurite Tracer (Longair et al., 2011) and a semi-automated tool for Fiji (Schindelin et al., 2012) in control NES cells, Pat1^{NES} , Pat2^{NES}, CCo1^{NES} and KO1^{NES} cells after 3 weeks of differentiation.

QUANTIFICATION AND STATISTICAL ANALYSIS

RNASeq and proteomics data analysis

Data analysis was performed with R (v3.3.2) (R Core Team (2013)), the supplementary code for statistical analysis and figures is provided. Mapped RNAseq count files were cleaned by removing all genes with raw counts of less than 3 per one million counts. Mapped proteins were only included if its peptides were detected across all samples. Data were then normalised on the total amount of reads per sample and statistically analysed with DESeq 2 (v1.14.1) of the Bioconductor tools without log2-fold change shrinkage (betaPrior = FALSE) by applying a Wald-test (Love et al., 2014). Adjusted p-values were calculated applying individual hypothesis weighting (Ignatiadis et al., 2016). Gene set enrichment analysis (GSEA) was performed on the Broad Institute GSEA Java platform against libraries (Subramanian et al., 2005), Hallmarks, KEGG, Biocarta, Reactome, all v5.2, which were also used to extract genes associated to OXPHOS-related pathways. Discrepancies of normalised enrichment scores between proteomic and transcriptomic GSEA data could be explained by the much larger sequencing depth of RNAseq (>13,237 accepted hits) compared to mass spectrometry (3058 accepted hits). Ontologies were identified

with WebGestalt (Wang et al., 2013). Human Gene Atlas comparisons were done in EnrichR (Kuleshov et al., 2016).

All parameters in our study were distributed normally. Experiments were performed at least three times when statistical tests applied. Data are expressed as mean ± standard deviation (SD) and differences were tested by a two-tailed t-test. The values $P < 0.05$ were considered statistically significant. Other types of analysis are indicated in the text. For confirmation of RNAseq or proteomics analysis experiments were repeated twice.

DATA AVAILABILITY

RNAseq raw data files and processed data are publicly available at GEO: GSE99559.

Proteomics raw data files and processed data are publicly available at PRIDE: PXD006647.

REFERENCES

Chambers, S.M., Fasano, C.A., Papapetrou, E.P., Tomishima, M., Sadelain, M., Studer, L., 2009. Highly efficient neural conversion of human ES and iPS cells by dual inhibition of SMAD signaling. Nat Biotechnol 27, 275–280. doi:10.1038/nbt.1529

Cong, L., Ran, F.A., Cox, D., Lin, S., Barretto, R., Habib, N., Hsu, P.D., Wu, X., Jiang, W., Marraffini, L.A., Zhang, F., 2013. Multiplex genome engineering using CRISPR/Cas systems. Science 339, 819–823. doi:10.1126/science.1231143

Falk, A., Koch, P., Kesavan, J., Takashima, Y., Ladewig, J., Alexander, M., Wiskow, O., Tailor, J., Trotter, M., Pollard, S., Smith, A., Brüstle, O., 2012. Capture of neuroepithelial-like stem cells from pluripotent stem cells provides a versatile system for in vitro production of human neurons. PLoS ONE 7, e29597. doi:10.1371/journal.pone.0029597

Haack, T.B., Ignatius, E., Calvo-Garrido, J., Iuso, A., Isohanni, P., Maffezzini, C., Lönnqvist, T., Suomalainen, A., Gorza, M., Kremer, L.S., Graf, E., Hartig, M., Berutti, R., Paucar, M., Svenningsson, P., Stranneheim, H., Brandberg, G., Wedell, A., Kurian, M.A., Hayflick, S.A., Venco, P., Tiranti, V., Strom, T.M., Dichgans, M., Horváth, R., Holinski-Feder, E., Freyer, C., Meitinger, T., Prokisch, H., Senderek, J., Wredenberg, A., Carroll, C.J., Klopstock, T., 2016. Absence of the Autophagy Adaptor SQSTM1/p62 Causes Childhood-Onset Neurodegeneration with Ataxia, Dystonia, and Gaze Palsy. Am. J. Hum. Genet. 99, 735–743. doi:10.1016/j.ajhg.2016.06.026

Ignatiadis, N., Klaus, B., Zaugg, J.B., Huber, W., 2016. Data-driven hypothesis weighting increases detection power in genome-scale multiple testing. Nat Meth 13, 577–580. doi:10.1038/nmeth.3885

Kim, D., Pertea, G., Trapnell, C., Pimentel, H., Kelley, R., Salzberg, S.L., 2013. TopHat2: accurate alignment of transcriptomes in the presence of insertions, deletions and gene fusions. Genome Biol 14, R36. doi:10.1186/gb-2013-14-4-r36

Koch, P., Opitz, T., Steinbeck, J.A., Ladewig, J., Bruestle, O., 2009. A rosette-type, self-renewing human ES cell-derived neural stem cell with potential for in vitro instruction and synaptic integration. Proc. Natl. Acad. Sci. U.S.A. 106, 3225–3230. doi:10.1073/pnas.0808387106

Kuleshov, M.V., Jones, M.R., Rouillard, A.D., Fernandez, N.F., Duan, Q., Wang, Z., Koplev, S., Jenkins, S.L., Jagodnik, K.M., Lachmann, A., McDermott, M.G., Monteiro, C.D., Gundersen, G.W., Ma'ayan, A., 2016.

Enrichr: a comprehensive gene set enrichment analysis web server 2016 update. Nucleic Acids Res. 44, W90–7. doi:10.1093/nar/gkw377

Longair, M.H., Baker, D.A., Armstrong, J.D., 2011. Simple Neurite Tracer: open source software for reconstruction, visualization and analysis of neuronal processes. Bioinformatics 27, 2453–2454. doi:10.1093/bioinformatics/btr390

Love, M.I., Huber, W., Anders, S., 2014. Moderated estimation of fold change and dispersion for RNA-seq data with DESeq2. Genome Biol 15, 550. doi:10.1186/s13059-014-0550-8

Schindelin, J., Arganda-Carreras, I., Frise, E., Kaynig, V., Longair, M., Pietzsch, T., Preibisch, S., Rueden, C., Saalfeld, S., Schmid, B., Tinevez, J.-Y., White, D.J., Hartenstein, V., Eliceiri, K., Tomancak, P., Cardona, A., 2012. Fiji: an open-source platform for biological-image analysis. Nat Meth 9, 676–682. doi:10.1038/nmeth.2019

Subramanian, A., Tamayo, P., Mootha, V.K., Mukherjee, S., Ebert, B.L., Gillette, M.A., Paulovich, A., Pomeroy, S.L., Golub, T.R., Lander, E.S., Mesirov, J.P., 2005. Gene set enrichment analysis: A knowledge-based approach for interpreting genome-wide expression profiles. Proc. Natl. Acad. Sci. U.S.A. 102, 15545–15550. doi:10.1073/pnas.0506580102

Wang, J., Duncan, D., Shi, Z., Zhang, B., 2013. WEB-based GEne SeT AnaLysis Toolkit (WebGestalt): update 2013. Nucleic Acids Res. 41, W77–83. doi:10.1093/nar/gkt439

Wibom, R., Hagenfeldt, L., Dobeln, von, U., 2002. Measurement of ATP production and respiratory chain enzyme activities in mitochondria isolated from small muscle biopsy samples. Anal. Biochem. 311, 139–151.

Wu, S., Johansson, J., Damdimopoulou, P., Shahsavani, M., Falk, A., Hovatta, O., Rising, A., 2014. Spider silk for xeno-free long-term self-renewal and differentiation of human pluripotent stem cells. Biomaterials 35, 8496–8502. doi:10.1016/j.biomaterials.2014.06.039